

Random-Anisotropy Blume-Emery-Griffiths Model

Amos Maritan,⁽¹⁾ Marek Cieplak,^{(2)(a),(3)} Michael R. Swift,⁽³⁾ Flavio Toigo,⁽¹⁾
and Jayanth R. Banavar^{(3)(a),(4)}

⁽¹⁾*Dipartimento di Fisica, Università di Padova, Padova 35131, Italy*

⁽²⁾*Polish Academy of Science, Warsaw, Poland*

⁽³⁾*Department of Physics and Materials Research Laboratory, Penn State University, 104 Davey Laboratory,
University Park, Pennsylvania 16802*

⁽⁴⁾*NEC Research Institute, Inc., 4 Independence Way, Princeton, New Jersey 08540*

(Received 1 April 1992)

We describe the results of studies of a random-anisotropy Blume-Emery-Griffiths spin-1 Ising model using mean-field theory, transfer-matrix calculations, and position-space renormalization-group calculations. The interplay between the quenched randomness of the anisotropy and the annealed disorder introduced by the spin-1 model leads to a rich phase diagram with a variety of phase transitions and reentrant behavior. Our results may be relevant to the study of the phase separation of ³He-⁴He mixtures in porous media in the vicinity of the superfluid transition.

PACS numbers: 05.50.+q

In recent years, there has been considerable interest in understanding the effects of randomness on phase transitions [1]. In this Letter, we study a model system with a novel interplay of quenched randomness and annealed disorder. A rich phase diagram is found including reentrant behavior, an example of order from disorder [2]. Our results are obtained using mean-field theory complemented by transfer-matrix and real-space renormalization-group calculations and are applicable to the phase separation of ³He-⁴He mixtures in aerogel [3] (an example of a porous medium) in the vicinity of the superfluid transition of ⁴He.

We study a Blume-Emery-Griffiths (BEG) [4-6] spin-1 model described by the Hamiltonian

$$H = -J \sum_{\langle ij \rangle} S_i S_j - K \sum_{\langle ij \rangle} S_i^2 S_j^2 + \sum_i \Delta_i S_i^2, \quad (1)$$

where $S_i = -1, 0, 1$ and $K = K_{33} + K_{44} - 2K_{34}$ with $K_{\alpha\beta}$ being the interaction energy between ${}^\alpha\text{He}$ - ${}^\beta\text{He}$ atoms ($\alpha, \beta = 3, 4$). Since $K_{\alpha\beta}$ is almost independent of α and β , the physically interesting case [4] corresponds to $K \sim 0$. Δ_i is a site-dependent field randomly distributed with a probability density $P(\Delta_i)$ on each site. For simplicity we choose

$$P(\Delta_i) = p\delta(\Delta_i - \Delta_0) + (1-p)\delta(\Delta_i - \Delta_1). \quad (2)$$

The spin states $S_i = \pm 1$ denote ⁴He and $S_i = 0$ ³He atoms with the superfluid transition corresponding to symmetry breaking between the ± 1 states. The fraction p of the sites with field Δ_0 corresponds to the pore-grain interface of aerogel and for the case that ⁴He ($S_i = \pm 1$) prefers to be at the interface, $\Delta_0 < 0$. (For simplicity, we ignore the grain space in our analysis.) Δ_1 is a bulk field that controls the total number of ³He ($S_i = 0$) atoms. Note that, unlike the random-field Ising model [1], the random field, here, does *not* break the \pm symmetry.

The mean-field approach entails the exact solution of

an infinite-range version of (1),

$$H = - \sum_{ij} \left[\frac{J}{N} S_i S_j + \frac{K}{N} S_i^2 S_j^2 \right] + \sum_i \Delta_i S_i^2. \quad (3)$$

The pore-grain interface of the aerogel is highly correlated. The infinite-range approximation may serve to capture the effects of such correlations. Following Schneider and Pytte [7], the quenched free energy density of (3) is given by

$$f = \frac{Jm^2}{2} + \frac{Kq^2}{2} - \frac{1}{\beta} \int d\Delta P(\Delta) \ln[1 + 2e^{\beta(Kq - \Delta)} \cosh(\beta Jm)], \quad (4)$$

where $m = \langle\langle S_i \rangle\rangle_\Delta$ and $q = \langle\langle S_i^2 \rangle\rangle_\Delta$ are the quenched averages of the equilibrium values of the two order parameters $\langle S_i \rangle$ and $\langle S_i^2 \rangle$ that minimize f . Setting the first derivative of f with respect to m and q equal to zero, one finds that $m = 0$ is always one solution with the corresponding value of q given by

$$q = \langle \delta^{-1} \rangle_\Delta \equiv \int d\Delta P(\Delta) \delta^{-1}, \quad (5)$$

where $\delta = 1 + e^{\beta(\Delta - Kq)}/2$. When m is nonzero,

$$q = m \coth(\beta Jm) \quad (6)$$

independent of the randomness, indicating that transitions take place in both q and m .

Setting $K = 0$, the zero-temperature phase diagram is shown in Fig. 1. There are four phases, labeled 1-4, with order parameters $m_1 = 1$, $m_2 = p$, $m_3 = 1 - p$, and $m_4 = 0$ and $q_i = m_i$, $i = 1, 4$. We focus on the region $\Delta_0 \lesssim 0$ allowing the zero-temperature phases 1 and 2. For $\Delta_1/J < (1+p)/2$, the entire system is magnetized at $T = 0$, i.e., filled with superfluid ⁴He whereas for $\Delta_1/J > (1+p)/2$, superfluidity occurs only at the pore walls with

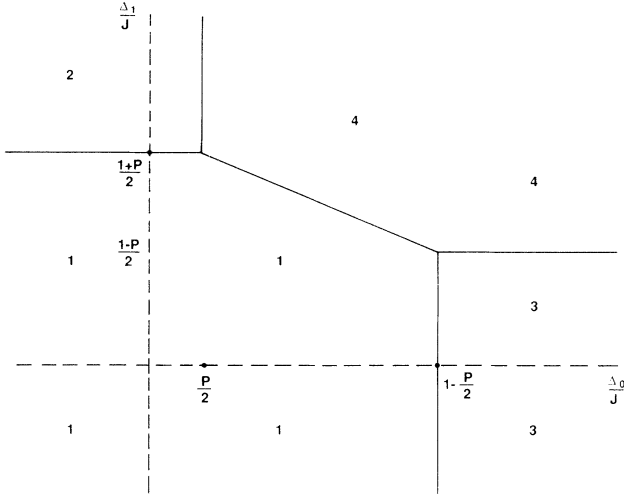


FIG. 1. $T=0$ phase diagram in the Δ_0/J - Δ_1/J plane.

^3He filling the interior of the pores. We will now proceed to study the behavior at nonzero temperatures.

Using Eq. (6) for the free energy, first-order transitions occur at the values of parameters such that $\text{Min}f(m, q) = f(m_1, q_1) = f(m_2, q_2)$ with $(m_1, q_1) \neq (m_2, q_2)$. A necessary condition for continuous transitions is that $\partial^n f / \partial m^n = 0$, $n=1, \dots, 2l-1$, $l \geq 2$ with $\partial^{2l} f / \partial m^{2l} > 0$ and q given by Eq. (6) for nonzero m . For $l=2$ and the $m=0$ case, $f(m)$ is even and $\partial f / \partial m = \partial^3 f / \partial m^3 = 0$. Setting $\partial^2 f / \partial m^2|_{m=0} = 0$, one finds

$$(\beta J)^{-1} = \langle \delta^{-1} \rangle_{\Delta}, \quad (7)$$

which on combining with Eq. (5) shows that *independent* of the disorder, the continuous transitions occurring at $m=0$ are given by

$$q = (\beta J)^{-1}. \quad (8)$$

For fixed Δ_0/T , K/T , and p , this corresponds to a line in the T/J - Δ_1/J plane. Noting also that $q=1-x$, where x is the concentration of ^3He , Eq. (8) predicts that in the T/J - x plane, the phase boundary is simply given by $T/J=1-x$ and is independent of the disorder. We have carried out an improved mean-field analysis [8] and find that contrary to the results of the simple approach, the phase boundary is indeed weakly dependent on the disorder. Further, the condition that $\partial^4 f / \partial m^4|_{m=0} > 0$ is equivalent to

$$\langle \delta^{-2} \rangle_{\Delta} - \frac{1}{3} \langle \delta^{-1} \rangle_{\Delta} > 0. \quad (9)$$

For the pure system ($p=0$), this condition reduces to

$$q = (\beta J)^{-1} > \frac{1}{3}. \quad (10)$$

Thus, a tricritical point would be present at $q_c = \frac{1}{3}$ if $\partial^6 f / \partial m^6|_{m=0, q=q_c} > 0$ and no first-order transition intervenes leading to a critical end point. Indeed, as pointed

out by Blume, Emery, and Griffiths [4], it is remarkable that the experimental q_c at which a tricritical point has been observed is 0.331 ± 0.005 .

Generic phase diagrams, predicted by the mean-field analysis, are shown in Fig. 2. The solid line denotes the continuous transition occurring at $T/J=q$, whereas the dashed line denotes the locus of coexistence where a first-order transition takes place. C is a critical point, and the points A and B are critical end points. [C is determined by setting the first three derivatives of f equal to zero and by solving for βJ , $\beta \Delta$, and $m \neq 0$ with the q - m relationship given by Eq. (6).] The inset of Fig. 2 shows the phase diagram for the case when Δ_0 is large and negative and p is not too small (e.g., $\Delta_0 = -3$, $p=0.3$). The first- and second-order lines miss each other. In this case, on decreasing the temperature from a large value, the ordering sets in through a continuous transition to a superfluid phase characterized by $m \neq 0$. On further cooling, a phase separation between $S^2=1$ and $S=0$ takes place through a first-order transition, unless one is at the critical concentration x_c .

We now turn to a discussion of the phase diagrams in Figs. 2(a) and 2(b). For specificity, we consider five possible paths labeled (1)–(5), each with a constant Δ_1/J . A similar (simpler) analysis can be readily carried out along constant ^3He concentration (x) trajectories. We begin by noting that the portions of the Δ_1/J axis $(0, (1+p)/2)$ and $((1+p)/2, \infty)$ are mapped onto the points $(T=0, x=0)$ and $(T=0, x=1-p)$ respectively in the x - T plane. The five trajectories are shown in both planes in Fig. 2. Let us consider following each of the trajectories increasing the temperature T from zero.

(1) At $T=0$, the ordered phase with $m=p$ and $q=1-x=p$ exists on a fraction p of the sites corresponding to the pore-grain interface, whereas the interior of the porous medium is filled with ^3He . On increasing the temperature, this ordering goes away as the trajectory crosses the line BD .

(2) The ground state has $m=q=1-x=1$, i.e., no ^3He is present. The trajectory crosses the phase transition lines 4 times on increasing the temperature. The first intersection is with the first-order line corresponding to a phase separation between ^3He and ^4He . In the resulting mixture, the ^4He is segregated near the aerogel and is superfluid whereas the ^3He jumps in concentration from $x \sim 0$ to $x \sim 1-p$ and fills the interior of the porous medium. On increasing the temperature further, the superfluidity near the aerogel is destroyed through intersection with the line BD . Reentrant behavior is found on increasing the temperature further. Thermal fluctuations cause the ^3He in the interior to be partly substituted by ^4He which undergoes a superfluid transition. A further increase in the temperature leads finally to a disordered state.

(3) The ground state is as in (2) above. On raising the temperature, the intersection with the first-order line

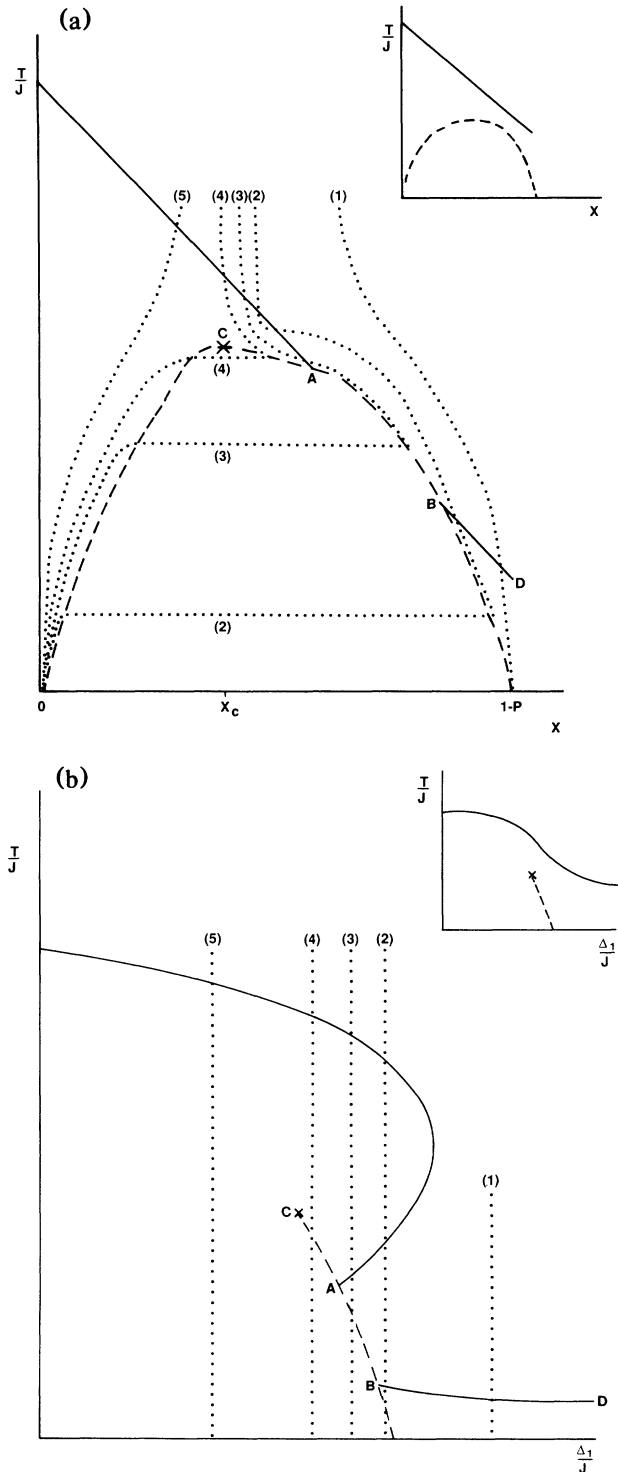


FIG. 2. Schematic phase diagrams for $\Delta_0 \leq 0$ in the (a) $x-T/J$ plane and (b) $\Delta_1/J-T/J$ plane. The dashed line denotes a first-order transition and the solid line a continuous transition. A and B are critical end points, and C a critical point. Insets: Representation of how the phase diagram is modified when Δ_0 is large and negative and p is large. The phase diagrams are *not* drawn to scale to enable easy viewing of the key features.

causes a transition to a normal fluid rich in ^3He . On further heating, as before, there is reentrance characterized by a superfluid phase that eventually disappears at an even higher temperature.

(4) At variance with (3) above, the first-order transition takes place entirely within an ordered phase—the jump in magnetization corresponds to a superfluid ^4He rich mixture replaced by a superfluid ^4He poor mixture. On further heating, the superfluidity is destroyed through a continuous transition.

(5) There is now only one transition at which the superfluidity goes continuously to zero.

The analysis so far has been based on an exact solution of an infinite-range model. The improved mean-field analysis [8] gives a nonzero percolation threshold ($p_c \sim 0.29$ in a simple cubic lattice) and the reentrant phenomenon is confirmed even when uncorrelated randomness is considered [9].

In order to confirm how well the mean-field predictions are qualitatively realized in low dimensions, we have carried out exact transfer-matrix calculations [9] in two dimensions for square systems containing up to 100 sites. We have also extended the position-space renormalization-group (PSRG) calculations of Berker and Wortis in two dimensions to the random case [9]. Briefly, an exact enumeration of all possible anisotropies is carried out and mapped into a renormalized bimodal distribution with effective p' , Δ'_0 , and Δ'_1 such that the three lowest moments of the actually obtained distribution and the effective bimodal distribution are equal [10]. Both the transfer-matrix and PSRG calculations are in qualitative accord with the mean-field predictions. There are two key differences: First, in $d=2$ for sufficiently small p ($p < p_c$) the line BD is missing since an ordered phase is not sustained by these sites. For the infinite-range model, p_c is effectively zero so that the line BD is present. Further, as in the BEG calculations, our calculations have dealt with Ising spins (and not xy spins). Thus the presence of line BD would be dependent on whether the pore-grain interface can sustain a superfluid phase. Second, studies of the BEG model with random bonds by Berker [11] have shown that randomness can have a profound effect on the nature of the phase transition in two dimensions. The prediction of this analysis is that symmetry-breaking first-order transitions such as line AB in Fig. 2(b) are converted to continuous transitions and non-symmetry-breaking first-order transitions [all other dashed lines in Fig. 2(b)] are completely eliminated. Our $d=2$ studies are in agreement with the latter prediction. We have not attempted to determine whether the transition is first order or not.

Our analysis should also be valid for the other physical systems described by the BEG model [6].

We are indebted to Moses Chan for suggesting that we tackle this problem and for many invaluable discussions. The work at Penn State was supported by NASA, NSF,

ONR, the Donors of the Petroleum Research Fund administered by the American Chemical Society, and by the Center for Academic Computing at Penn State. The work at Padova was supported by the Italian Ministero dell'Università through INFM (consorzio Interuniversitario di Fisica della Materia). The work at Poland was supported by the Polish KBN. A.M. and J.R.B. acknowledge the support provided by a NATO travel grant.

^(a)Permanent address.

- [1] D. S. Fisher, G. Grinstein, and A. Khurana, *Phys. Today* **41**, No. 12, 58 (1988).
- [2] J. Villain, R. Bidaux, J. P. Carton, and R. Conte, *J. Phys. (Paris)* **41**, 1263 (1976).
- [3] Such experiments are currently underway in the laboratories of Moses Chan at Penn State University.
- [4] M. Blume, V. J. Emery, and R. B. Griffiths, *Phys. Rev. A* **4**, 1071 (1971).
- [5] A. N. Berker and M. Wortis, *Phys. Rev. B* **14**, 4946 (1976).
- [6] W. Hoston and A. N. Berker, *Phys. Rev. Lett.* **67**, 1027 (1991); the references therein discuss applications of the BEG model to solid-liquid-gas systems, multicomponent fluid and liquid crystal mixtures, microemulsions, and alloys. X. P. Jiang and M. R. Giri, *J. Phys. C* **21**, 995 (1988).
- [7] T. Schneider and E. Pytte, *Phys. Rev. B* **15**, 1519 (1977); D. Sherrington, *Phys. Lett.* **58A**, 36 (1976).
- [8] R. R. Netz and A. N. Berker, *Phys. Rev. Lett.* **66**, 377 (1991); **67**, 1808 (1991); J. R. Banavar, M. Cieplak, and A. Maritan, *Phys. Rev. Lett.* **67**, 1807 (1991).
- [9] Details will be published elsewhere.
- [10] J. M. Yeomans and R. B. Stinchcombe, *J. Phys. C* **12**, 347 (1979).
- [11] K. Hui and A. N. Berker, *Phys. Rev. Lett.* **62**, 2507 (1989); A. N. Berker, *J. Appl. Phys.* **70**, 5941 (1991); see also M. Aizenman and J. Wehr, *Phys. Rev. Lett.* **62**, 2503 (1989).